Corticotropin-releasing factor receptor 2 is a tonic suppressor of vascularization

Tracy L. Bale*†, Frank J. Giordano†‡, Reed P. Hickey‡, Yan Huang‡, Anjali K. Nath‡, Kirk L. Peterson§, Wylie W. Vale*, and Kuo-Fen Lee*¶

*Clayton Foundation Laboratories for Peptide Biology, The Salk Institute, La Jolla, CA 92037; ‡Yale University School of Medicine, New Haven, CT 06510; and §School of Medicine, University of California at San Diego, La Jolla, CA 92093

Contributed by Wylie W. Vale, March 29, 2002

Angiogenesis is regulated by means of a balance between activators and inhibitors. However, little is known regarding the regulation of the quiescent state of adult vessels. Corticotropin-releasing factor receptor 2 (CRFR2) is found in both endothelial and smooth muscle cells (SMCs) in the vasculature, where its function has remained elusive. We have investigated the role of CRFR2 as a determinant of tissue vascularization by comparing control and CRFR2-deficient mice with immunohistological and morphometric techniques. To define the mechanisms responsible for CRFR2 inhibition of angiogenesis, we have also examined *in vitro* the effect of ligand activation on cell proliferation, cell cycle protein phosphorylation, and capillary tube formation. Our results demonstrate that mice deficient for CRFR2 become hypervascularized postnatally. Activation of this receptor *in vitro* results in reduced vascular endothelial growth factor (VEGF) release from SMCs, an inhibition of SMC proliferation, and inhibition of capillary tube formation in collagen gels. Treatment of a subcutaneously injected gel matrix with a CRFR2 agonist inhibits growth factor-induced vascularization. Western blots show that cell cycle retinoblastoma protein, which is essential for cell cycle progression, is decreased by CRFR2 agonist treatment in SMCs. These results suggest that CRFR2 is a critical component of a pathway necessary for tonic inhibition of adult neovascularization. CRFR2 may be a potential target for therapeutic modulation of angiogenesis in cancer and ischemic cardiovascular disease.

Angiogenesis is regulated by a balance between activators and inhibitors. Whereas adult neovascularization is normally limited to sites of wound healing and malignancy (1), transgenic mice overexpressing angiogenic factors such as vascular endothelial growth factor (VEGF) or angiopoietin demonstrate that increased vascularization in normal nonischemic tissue can occur under stimulatory conditions (2, 3). Inhibitors of angiogenesis have been shown to be important regulators during neovascularization in development and in tumor formation. Factors such as vascular endothelial growth inhibitor (VEGI), angiostatin, or pigment epithelium-derived factor can inhibit tumor growth by suppressing vascularization (4–6). While these inhibitory factors have been shown to be important for normal vascular development, little is known regarding the regulation of the quiescent state of adult vessels.

Corticotropin-releasing factor (CRF) and its family of ligands including urocortin I (UcnI), UcnII (also known as stresscopin-related peptide), and UcnIII (also known as stresscopin) are found in the periphery as well as in the central nervous system. While CRF is a critical coordinator of the hypothalamic–pituitary–adrenal axis in response to stress, it has also been shown to activate the sympathetic nervous system as well as to promote anxiety-like behaviors (7–9). Central administration of CRF elevates blood pressure and heart rate, whereas peripheral administration of CRF or UcnI results in vasodilation and a decrease in blood pressure (10, 11). The CRF family of ligands function by activation of their two known receptors, CRFR1 and CRFR2 (12–16). These receptors are G-protein coupled, and their activation results in elevated cAMP levels and activation of cAMP-dependent protein kinase (PKA). These ligands differ in their localization as well as their affinity for the CRF receptors. Whereas CRF has a 10-fold higher affinity for CRFR1 than for CRFR2, UcnI has equal affinity for both receptors (17). The more recently identified ligands, UcnII and UcnIII, are specific for CRFR2 (18–20). Both CRFR1 and CRFR2 are expressed in the central nervous system and periphery. In the periphery, CRFR2 is expressed in cardiac myocytes and in the systemic vasculature. The peripheral vasodilation seen after infusion of CRF or UcnI has been attributed to activation of CRFR2, found in both endothelial cells (ECs) and smooth muscle cells (SMCs) of the blood vessel (21–26). To examine the endogenous role of CRFR2, we have investigated its action as a determinant of tissue vascularization. Using immunohistochemistry and sensitive morphometric techniques, we have quantifiably compared vascularization of *CRFR2*-mutant and control mice. Further, we have examined *in vitro* the possible mechanisms of CRFR2 inhibition of angiogenesis.

Methods

Whole-Mount Immunostaining. Tissues were taken from embryos removed at day 11, or postnatal days 2, 10, and 15 ($n = 4$) and fixed in 4% paraformaldehyde for 2 days. Tissues were then bleached in Dent's fixative (4:1, vol/vol, methanol/DMSO) plus 5% hydrogen peroxide overnight at 4°C, washed in 1× TBS (50 mM Tris·HCl, pH 7.5/150 mM NaCl) plus 1% Tween-20, three times for 30 min each, and blocked with 5% goat serum in dilution buffer (0.5 M NaCl/0.01 M PBS/3.0% BSA/0.3% Triton X-100) plus 1% DMSO overnight at room temperature (RT). Platelet–endothelial cell adhesion molecule (PECAM) antibody was added (PharMingen, 1:1000) to the blocking mix and incubated for 2 days at RT. Tissues were then washed in 1× TBS plus 1% Tween-20 and 1% DMSO, three times for 1 h each. Secondary incubation (goat anti-rat horseradish peroxidase, 1:5000) was carried out overnight at RT. Tissue was washed as before. A final wash in 1× TBS was done for 1 h. The peroxide reaction was carried out by glucose oxidase (Calbiochem) reaction mix incubated with tissue until an orange-brown color developed. Tissue was dehydrated in a methanol series and water was replaced with glycerol for clearing.

Microfil Polymer Perfusion. Microfil (Flow Tech, Carver, MA) perfusion was conducted by using a syringe pump and a 30 gauge needle placed in the left ventricle of the heart of anesthetized animals ($n = 4$). The right atrium was opened to serve as a drain vent. The process was continued until the perfusate drained freely from the atrial vent. The animals were then placed at 4°C overnight to allow the polymer to cure. Specimens were dissected from the cured animals and dehydrated through an ethanol series: 25% day

Abbreviations: VEGF, vascular endothelial growth factor; CRF, corticotropin-releasing factor; CRFR, CRF receptor; Ucn, urocortin; EC, endothelial cell; SMC, smooth muscle cell; PECAM, platelet–endothelial cell adhesion molecule; Rb, retinoblastoma protein; bFGF, basic fibroblast growth factor.

†T.L.B. and F.J.G. contributed equally to this work.

¶To whom correspondence and requests for materials should be addressed at: Clayton Foundation Laboratories for Peptide Biology, The Salk Institute, 10010 N. Torrey Pines Rd., La Jolla, CA 92037. E-mail: klee@salk.edu.

 www.pnas.org/cgi/doi/10.1073/pnas.102187099

1, 50% day 2, 75% day 3, 95% day 4, 100% day 5. Tissues were also bleached with 6% hydrogen peroxide on day 2. After dehydration, tissues were cleared in glycerol. For quantification of weight of vascular casts, perfused tissues were digested with proteinase K (10 μg/ml) overnight at 55°C. All tissues were identical in weight before digestion. After digestion, remaining Microfil casts were rinsed, dried, and weighed. For quantification of vessel numbers in cerebral cortex, perfused brains were embedded in gelatin/albumin and sectioned (25 μm in thickness) on a Vibratome. Four identical cortical regions were analyzed for each animal ($n = 3$), and results were averaged. Vessel numbers were obtained by manually counting vessels within a fixed unit area [a 1.5 × 1.5 inch (38 × 38 mm) square] for all tissue sections in a high-resolution digital color camera enlarged image of each tissue section. For quantification of the cross-sectional diameter of large conductance vessels, images were enlarged by using the digital camera as described above. Four measurements per animal were taken for cerebral vessels and small intestine ($n = 3$). For the kidney, the diameter of the renal artery immediately preceding vessel entrance into the kidney was measured for each animal ($n = 3$). All data are reported as the mean for each group ± SE.

Western Blot Analysis. For comparison of levels of phosphorylated retinoblastoma protein (Rb), SMCs were serum starved for 24 h before 24 h of Ucn treatment. Cells were then harvested for protein extracts. For comparison of VEGF levels, tissues were taken from control and CRFR2-mutant mice. Cells and tissues were homogenized in buffer (50 mM Tris·HCl, pH 7.4/1 mM DTT/2 mM $MgCl_2$/1 mM EDTA/0.5 mM PMSF/5 μg/ml leupeptin/2 μg/ml aprotinin). Protein extracts (40 μg per lane as determined by Bradford assay for protein content) were separated by SDS/10% PAGE (Novex, San Diego) and transferred to a nitrocellulose membrane. Blots were blocked in 5% nonfat dry milk for 1 h, washed in 1× TBS plus 0.2% Tween-20 (TBST), incubated with anti-VEGF antibody (1:1000; Santa Cruz Biotechnology) or anti-phosphorylated Rb antibody (1:1000; Cell Signaling Technologies, Beverly, MA) 1 h, washed in TBST twice for 20 min each, incubated with horseradish peroxidase-conjugated anti-rabbit IgG (1:10,000; Amersham) 1 h, and washed in TBST twice for 20 min. Blots were visualized with ECL reagent (Amersham Pharmacia).

VEGF Production. Rat vascular SMCs plated at equal density on 6-cm tissue culture plates were treated with either Ucn (100 nM) or vehicle control. Twenty-four hours after treatment the conditioned medium was collected from each plate and the cells were washed and scraped into lysis buffer. VEGF concentration in the conditioned medium was determined by a sensitive ELISA (Quantikine M; R & D Systems). Protein content of cell lysates was determined by a standard Bradford assay.

Proliferation Assay. SMCs were treated for 48 h with Ucn (1 nM, 10 nM, 50 nM, 100 nM, 500 nM, or 1 μM). Proliferation was assessed by a microtiter plate assay method (CellTiter 96; Promega). This assay is based on the cellular reduction of a tetrazolium salt to a formazan product and correlates closely with analysis of proliferation by [^{3}H]thymidine incorporation. SMCs were serum starved for 24 h before treatment. Results were determined on an ELISA plate reader at 570 nm.

Capillary Tube Formation *in Vitro*. The three-dimensional collagen gel assay was performed with rat aortic ECs suspended in a mixture of 2.5 mg/ml rat tail type I collagen. The matrix solution was added to M199 culture medium supplemented with 150 mM Hepes, adjusted to pH 7.4 with sodium bicarbonate. Drops of 0.2 ml of the mixture of cells and matrix were pipetted onto six-well plates and allowed to solidify at 37°C for 30 min. Growth medium supplemented with either rat VEGF plus vehicle or VEGF plus 1 μM Ucn was replenished daily. On day 4, phase-contrast pictures were taken and the gel drops were removed and embedded in OCT. For quantification, gels were sectioned and fixed in acetone and immunofluorescence with 4′,6-diamidino-2-phenylindole (DAPI) was measured. Cell counts were performed on three different sections for each treatment.

***In Vivo* Matrigel Matrix Assay.** To evaluate the ability of Ucn to modulate the vascularization within a gel matrix, growth factor-reduced Matrigel (Collaborative Research, Becton Dickinson, Bedford, MA; 600 μl) containing heparin (20 units) and either basic fibroblast growth factor (bFGF; Sigma, 20 ng) or bFGF and Ucn (1 μg) was subcutaneously injected into the hind flanks of wild-type mice. Before injection, mice were lightly anesthetized and their flanks were shaved. The Matrigel was kept on ice in cold syringes before injection and immediately solidified upon injection. Plugs were removed after 3 days, fixed in formalin, and embedded in paraffin. Gel sections (10 μm in thickness) were then stained with hematoxylin and eosin.

Results and Discussion

Hypervascularization of CRFR2-Deficient Mice. These studies revealed a profound increase in blood vessel density in adult *CRFR2*-mutant mice. To determine at what stage of development this hypervascularization occurs, tissues from control and *CRFR2*-mutant mice were whole-mount immunostained for PECAM. Comparisons of all tissues examined showed no differences in blood vessel density at embryonic day 11 (Fig. 1 *a* and *b*) or postnatal day 15 (Fig. 1 *c* and *d*). Microfil high-resolution vascular casts demonstrated that the increased vessel density occurs by postnatal day 21 (Fig. 1 *e* and *f*) and is also seen in adults (Fig. 1 *g–l*). PECAM whole-mount immunostaining of adult tissues also shows the hypervascularization of *CRFR2*-mutant mice (data not shown). To quantify the hypervascularization in the *CRFR2*-mutant mice, Microfil-perfused tissues were digested with proteinase K (Fig. 2 *a* and *b*). Tissue-digested Microfil casts from *CRFR2*-mutant mouse tissues weigh significantly more than casts from control mouse tissues (Fig. 2*c*). Start weights of the tissues before proteinase K digestion were not different (kidney: control 1.1 ± 0.09 g, knockout 1.1 ± 0.04 g; stomach: control 1.0 ± 0.04 g, knockout 0.99 ± 0.04 g; gastrointestinal tract: control 0.98 ± 0.02 g, knockout 0.98 ± 0.03 g). Comparison of the cross-sectional diameter of the large conductance vessels for each tissue revealed significant increases in vessel size in the *CRFR2*-mutant mice (Fig. 2*d*). Microfil-perfused tissues were also fixed and sectioned to better compare tissue vascularization and size (Fig. 2 *e–j*). Brain cortical sections were quantified for vessel numbers for each animal and revealed significantly more vessels in the *CRFR2*-mutant mice than in similar cortical regions in controls (Fig. 2*k*). These findings suggest a possible role for CRFR2 as a regulator of tissue vascularity, as in its absence vessel number and size are increased. Thus, CRFR2 signaling may represent a previously unrecognized pathway of tonic vascular inhibition that differs from pathways involving other known inhibitory factors. Interestingly, despite a much larger vascular surface area, *CRFR2*-mutant mice are also hypertensive (27). Although the mechanism of this hypertension is not currently known, it is possibly related to an increase in the number of peripheral small resistance vessels in these mice in conjunction with a loss of tonic vasodilatory effects of CRFR2 ligands.

CRFR2 Regulation of VEGF. To gain insight into the mechanism whereby the absence of CRFR2 results in increased vascularization, tissues from control and mutant mice were analyzed by Western blotting for VEGF content. VEGF, as an EC-specific mitogen and a major mediator of pathological angiogenesis, is required for survival, as mice deficient for even one allele of this gene die during development (28, 29). Western blot analysis of brown and white adipose tissues and pituitary gland demonstrated increased VEGF levels in tissues from *CRFR2*-mutant mice (Fig. 3*a*). To further

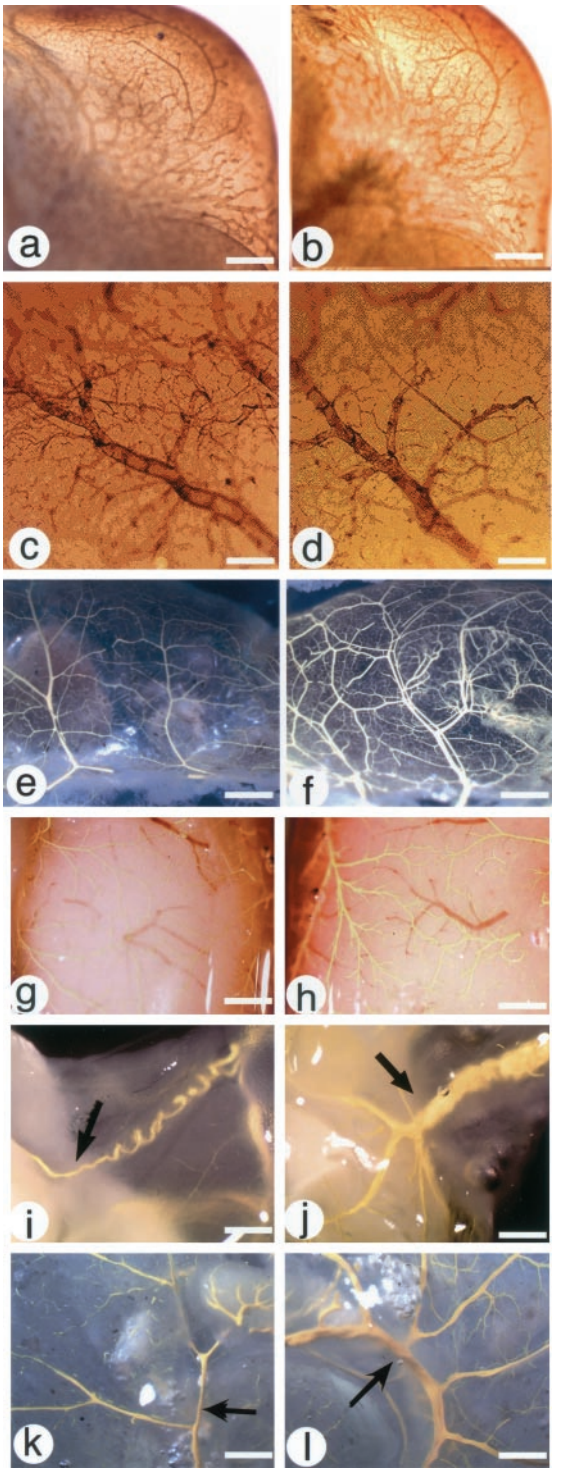

Fig. 1. Hypervascularization of *CRFR2*-mutant mice. (*a–d*) Whole-mount immunocytochemistry of PECAM-immunostained tissues from embryonic day 11 CRFR2 control (*a*) and mutant (*b*) mouse head (scale bar represents 0.8 mm) and from postnatal day 15 *CRFR2* control (*c*) and mutant (*d*) mouse brain (scale bar represents 0.08 mm), showing no differences in vessel density. (*e* and *f*) Microfil-perfused tissues from 3-week-old *CRFR2* control (*e*) and mutant (*f*) mouse small intestine, showing increased vessel numbers in the mutant mouse (scale bar represents 0.75 mm). (*g–l*) Microfil-perfused tissues from adult *CRFR2* control (*g*, *i*, and *k*) and mutant (*h*, *j*, and *l*) mice, showing increased vessel density in the mutant mouse in the dorsal brain surface (*g* and *h*; scale bar represents 0.45 mm), testicular artery (*i* and *j*; scale bar represents 1.4 mm), and large intestine (*k* and *l*; scale bar represents 2.5 mm). Arrows indicate testicular artery (*i* and *j*) and mesenteric artery (*k* and *l*).

examine the effect of CRFR2 activation on VEGF production, rat SMCs were treated for 24 h with the CRFR2 agonist Ucn. After treatment, VEGF levels were measured by ELISA. Results show a significant decrease in detectable VEGF after the Ucn treatment (vehicle 414.22 ± 7.4 pg/ml, Ucn 384.04 ± 8.2 pg/ml; $P < 0.01$), suggesting possible involvement of CRFR2 in modulation of VEGF production. Even small alterations in VEGF levels can result in dramatic changes in vascularity, as demonstrated by the profound phenotype and embryonic lethality in mice deficient for even one VEGF allele (28, 29). Therefore, loss of CRFR2 suppression of VEGF expression could be a contributing mechanism by which hypervascularization occurs in the *CRFR*-mutant mice.

CRFR2 Inhibition of Cellular Proliferation. To further elucidate the mechanism whereby CRFR2 activation may inhibit blood vessel growth, we examined the effect of Ucn treatment on SMC proliferation and EC tube formation. SMCs were treated with Ucn and assayed for effects on cellular proliferation. These studies reveal a dose-responsive and significant inhibition of SMC proliferation by Ucn (Fig. 3*b*). Terminal deoxynucleotidyltransferase-mediated dUTP end labeling (TUNEL)-positive staining for detection of apoptosis did not reach a level beyond background for basal or Ucn treatment, indicating that the Ucn-induced decrease in proliferation was not a result of increased cell death (data not shown).

CRFR2 Inhibition of the Cell Cycle. To determine the possible mechanism whereby activation of CRFR2 may inhibit cell proliferation, we examined by Western blot the expression of the cell cycle protein Rb in SMCs after Ucn treatment. Rb is the product from a retinoblastoma tumor suppressor gene and functions as the checkpoint at which DNA damage is caught. In rapidly proliferating cells, Rb is highly phosphorylated; it is in its least phosphorylated state in resting cells (30). We found that Ucn treatment dose dependently decreased the phosphorylation of Rb (Fig. 3*f*). These results support the role of CRFR2 as an inhibitor of cell proliferation, as decreased levels of Rb phosphorylation indicate increased inhibition of the cell cycle.

Ucn Inhibition of Angiogenesis. Ucn treatment also inhibits the VEGF-stimulated formation of capillary-like tubes in three-dimensional collagen gels containing rat aortic ECs (Fig. 3 *c* and *d*). Formation of elongated, bifurcating tubules that pervade the gel matrix (Fig. 3 *c1* and *d1*) were inhibited with the addition of Ucn (Fig. 3 *c2* and *d2*). A decrease in the number and size of tubules as well as the number of branches formed was observed. Quantification of EC number in gel sections shows significantly fewer cells in the Ucn-treated gels (Fig. 3*e*). To examine Ucn effects on *in vivo* vascularization, we subcutaneously injected Matrigel (a basement membrane matrix) containing bFGF that induced formation of an intricate network of vessels within 3 days in mice (Fig. 3 *g1*). However, treatment of the gel with Ucn in addition to bFGF completely inhibited this vascularization (Fig. 3 *g2*). Fixed and stained Matrigels recovered from these animals showed endothelial cell migration, and large capillaries formed in the bFGF gels (Fig. 3 *g3*), whereas no cells or vessels were detected in the Ucn-treated gel sections (Fig. 3 *g4*).

These results support the hypothesis that the endogenous role of vascular CRFR2 may be inhibition of proliferation, possibly by means of an effect on the endothelial cell cycle, and/or an indirect effect by means of a modulation of SMC VEGF production. Actions of CRFR2 ligands have been shown to produce a multitude of effects involving the peripheral vasculature, including vasodilation and sustained hypotension (17, 23, 25, 31–33). Ucn administration elevates cardiac contractility in conscious animals (34) and inhibits heat-induced edema (35). Interestingly, CRF, which is a CRFR1-selective ligand having 10-fold lower affinity for CRFR2, has been shown to stimulate endothelial cell chemotaxis and enhance angiogenesis in epithelial-cell tumors (36). While these

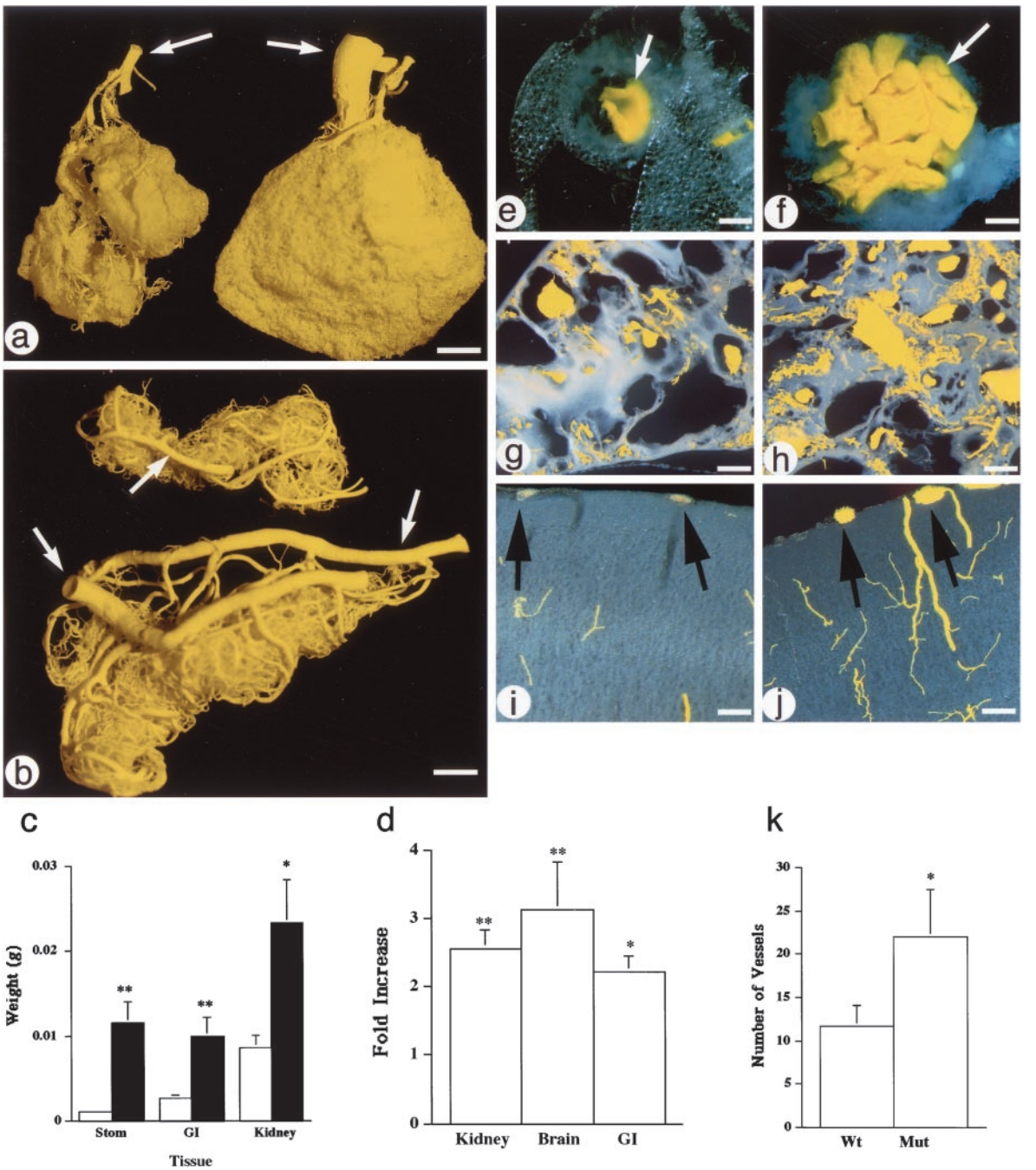

Fig. 2. Quantification of hypervascularization of *CRFR2*-mutant tissues. (*a* and *b*) Microfil casts after tissue digestion of *CRFR2* control and mutant tissues. (*a*) Kidney, control is on left, *CRFR2* mutant is on right (arrows indicate renal artery). (*b*) Intestine, control is on top, *CRFR2* mutant is on bottom (arrows indicate mesenteric artery). (Scale bars represent 0.5 mm.) (*c* and *d*) Quantification of Microfil casts for comparison of weight of tissues (*c*) from *CRFR2* control (white bars) or mutant (black bars) mice after proteinase K digestion, and cross-sectional diameter (*d*) of large conductance vessels showing fold increase in size of *CRFR2*-mutant vessels compared with control vessels. For the kidney, the renal artery was measured; for the gastrointestinal (GI) tract, the mesenteric artery was measured; and for the brain, the cerebral surface vessels were measured. Stom, stomach. Data are mean ± SEM; $n = 3$; ∗, $P < 0.05$; ∗∗, $P < 0.01$. (*e–j*) Sectioned tissues of Microfil casts for testicular artery (*e* and *f*), spleen (*g* and *h*), and cerebral cortex (*i* and *j*), showing increased vascular density in the *CRFR2*-mutant mice (*f*, *h*, and *j*) compared with control (*e*, *g*, and *i*). Arrows indicate cerebral vessels in CRFR2 control (*i*) and mutant (*j*) mouse brains, demonstrating increased size in *CRFR2* mutant mice. (Scale bars represent 0.2 mm.) (*k*) Quantification of vessel counts in cerebral cortex. Wt, wild type; Mut, *CRFR2* mutant. Data are mean ± SEM; $n = 3$; ∗, $P < 0.05$.

effects are in opposition to results shown here, the action for CRF may be through a different receptor or mechanism than that occurring through CRFR2 activation.

Effects of CRFR2 activation on vascularization are of particular interest for therapeutic modulation of angiogenesis. The increased vascularity observed in the *CRFR2*-mutant mice involves not only an increase in tissue capillaries but also a profound increase in both the size and number of larger conductance vessels. These larger conduits are likely to be particularly important to the success of stimulated angiogenesis in the treatment of ischemic tissue beds, wherein the problem is not a decrease in local capillarization, but rather a loss of tissue perfusion because of decreased large vessel

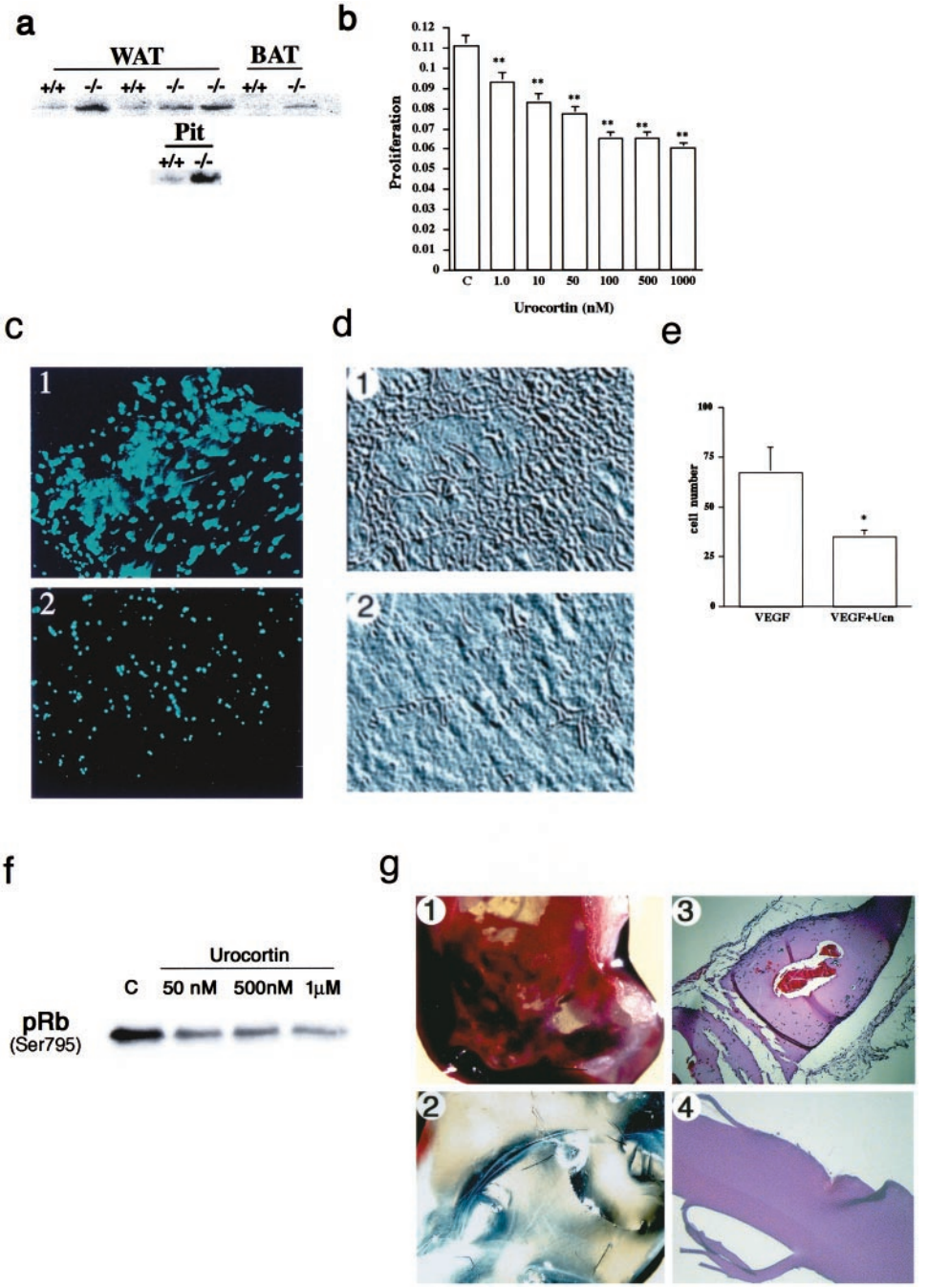

Fig. 3. Mechanism of CRFR2 inhibition of vascularization. (*a*) Western blot showing increased VEGF expression in white (WAT) and brown (BAT) adipose tissue and pituitary gland (Pit) from *CRFR2*-mutant mice. Figure is a representative of three repeated experiments. (*b*) Inhibition of SMC proliferation and capillary tube formation with Ucn treatment. SMCs treated for 48 h with Ucn demonstrated a dose-responsive and significant inhibition of SMC proliferation. C, control. Data are expressed as mean ± SEM, $n = 20$; **, $P < 0.001$. (*c–e*) Ucn treatment also inhibited the formation of capillary-like tubes in three-dimensional collagen gels containing rat aortic endothelial cells. Formation of elongated bifurcating tubules that pervaded the gel matrix (*c1* and *d1*) was inhibited with Ucn treatment, as a decrease in the number and size of tubules formed was seen (*c2* and *d2*). (*c*) 4′,6-Diamidino-2-phenylindole (DAPI) immunofluorescence of ECs in sections from collagen gels, treated with VEGF (*1*) or VEGF plus Ucn (*2*). (×10.) (*d*) Phase-contrast images from collagen gels, treated with VEGF (*1*) or VEGF plus Ucn (*2*). (×10.) (*e*) Quantification of cell numbers in gel sections after treatment. Data are expressed as mean ± SEM, $n = 3$; *, $P < 0.05$. (*f*) Western blot showing a dose-responsive decrease in phosphorylation of Rb in SMCs after Ucn treatment. Cells were treated for 24 h before harvest. C, control. (*g*) Matrigel plugs demonstrating immense vascularization in the bFGF treatment (*1*) and no vascularization in the Ucn and bFGF treatment (*2*). (*3* and *4*) Hematoxylin and eosin-stained sections from *1* and *2*, respectively showing capillary formation and EC migration (blue-stained nuclei) in the bFGF treatment (*3*) and inhibition of vessel formation and migration in the Ucn and bFGF treatment (*4*). (×10.)

conductance. Also of significant interest are the results showing that the hypervascularity in the *CRFR2*-mutant mice does not occur in early development, but appears to be a progressive process continuing into adulthood. This observation supports the premise of stimulated therapeutic angiogenesis and suggests that under optimal circumstances marked increases in both large and small vessels can be induced in established vascular beds. This previously undescribed role for CRFR2 may present the field of therapeutic

angiogenesis with a mechanism by which vessel densities can be increased not only in number, but also in size; providing a potential major advantage over current strategies now being tested in clinical trials (37–39).

In summary, *CRFR2*-mutant mice are hypervascularized. CRFR2 activation inhibits SMC proliferation as well as EC tube formation *in vitro*, and also inhibits growth factor-induced vascularization of a Matrigel matrix *in vivo*. The Ucn-stimulated decrease in phosphorylated Rb demonstrates a direct action of CRFR2 on inhibition of cell proliferation. Together, results from these studies demonstrate a critical role for CRFR2 in tonic regulation of angiogenesis and remodeling of the juvenile and adult vasculature, suggesting that CRFR2 may be a potential new target to modulate angiogenesis in diseases such as cancer or ischemic cardiovascular disease.

We thank S. Guerra for help with the manuscript, K. Creehan for animal assistance, and K. Anderson for technical assistance. This work was supported in part by grants from the National Institutes of Health (DK 26741), the Robert J. and Helen C. Kleberg Foundation, the Adler Foundation, the Ludwick Family Foundation, the Foundation for Research, and the Foundation for Medical Research, Inc. T.L.B. is supported by a National Research Service Award. F.J.G. is supported by Grant AHA9730083N from the American Heart Association.

1. Engerman, R. L., Pfaffenbach, D. & Davis, M. D. (1967) *Lab. Invest.* **17,** 738–743.
2. Miller, J. W. (1997) *Am. J. Pathol.* **151,** 13–23.
3. Suri, C., McClain, J., Thurston, G., McDonald, D. M., Zhou, H., Oldmixon, E. H., Sato, T. N. & Yancopoulos, G. D. (1998) *Science* **282,** 468–471.
4. O'Reilly, M. S., Pirie-Shepherd, S., Lane, W. S. & Folkman, J. (1999) *Science* **285,** 1926–1928.
5. Zhai, Y., Ni, J., Jiang, G. W., Lu, J., Xing, L., Lincoln, C., Carter, K. C., Janat, F., Kozak, D., Xu, S., *et al*. (1999) *FASEB J.* **13,** 181–189.
6. Dawson, D. W., Volpert, O. V., Gillis, P., Crawford, S. E., Xu, H., Benedict, W. & Bouck, N. P. (1999) *Science* **285,** 245–248.
7. Brown, M. R., Fisher, L. A., Spiess, J., Rivier, C., Rivier, J. & Vale, W. (1982) *Endocrinology* **111,** 928–931.
8. Koob, G. F. & Thatcher-Britton, K. (1985) *Prog. Clin. Biol. Res.* **192,** 499–506.
9. Britton, K. T., Lee, G., Vale, W., Rivier, J. & Koob, G. F. (1986) *Brain Res.* **369,** 303–306.
10. Brown, M. R., Fisher, L. A., Spiess, J., Rivier, J., Rivier, C. & Vale, W. (1982) *Regul. Pept.* **4,** 107–114.
11. Fisher, L. A., Rivier, J., Rivier, C., Spiess, J., Vale, W. & Brown, M. R. (1982) *Endocrinology* **110,** 2222–2224.
12. Chen, R., Lewis, K. A., Perrin, M. H. & Vale, W. W. (1993) *Proc. Natl. Acad. Sci. USA* **90,** 8967–8971.
13. Kishimoto, T., Pearse, R. V., 2nd, Lin, C. R. & Rosenfeld, M. G. (1995) *Proc. Natl. Acad. Sci. USA* **92,** 1108–1112.
14. Perrin, M., Donaldson, C., Chen, R., Blount, A., Berggren, T., Bilezikjian, L., Sawchenko, P. & Vale, W. (1995) *Proc. Natl. Acad. Sci. USA* **92,** 2969–2973.
15. Stenzel, P., Kesterson, R., Yeung, W., Cone, R. D., Rittenberg, M. B. & Stenzel-Poore, M. P. (1995) *Mol. Endocrinol.* **9,** 637–645.
16. Chalmers, D. T., Lovenberg, T. W. & De Souza, E. B. (1995) *J. Neurosci.* **15,** 6340–6350.
17. Vaughan, J., Donaldson, C., Bittencourt, J., Perrin, M. H., Lewis, K., Sutton, S., Chan, R., Turnbull, A. V., Lovejoy, D., Rivier, C., *et al*. (1995) *Nature (London)* **378,** 287–292.
18. Reyes, T. M., Lewis, K., Perrin, M. H., Kunitake, K. S., Vaughan, J., Arias, C. A., Hogenesch, J. B., Gulyas, J., Rivier, J., Vale, W. W. & Sawchenko, P. E. (2001) *Proc. Natl. Acad. Sci. USA* **98,** 2843–2848.
19. Lewis, K., Li, C., Perrin, M. H., Blount, A., Kunitake, K., Donaldson, C., Vaughan, J., Reyes, T. M., Gulyas, J., Fischer, W., *et al*. (2001) *Proc. Natl. Acad. Sci. USA* **98,** 7570–7575.
20. Hsu, S. Y. & Hsueh, A. J. (2001) *Nat. Med.* **7,** 605–611.
21. Iwakiri, Y., Chijiiwa, Y., Motomura, Y., Osame, M. & Nawata, H. (1997) *Life Sci.* **60,** 857–864.
22. Fleisher-Berkovich, S., Rimon, G. & Danon, A. (1998) *Eur. J. Pharmacol.* **353,** 297–302.
23. Schilling, L., Kanzler, C., Schmiedek, P. & Ehrenreich, H. (1998) *Br. J. Pharmacol.* **125,** 1164–1171.
24. Simoncini, T., Apa, R., Reis, F. M., Miceli, F., Stomati, M., Driul, L., Lanzone, A., Genazzani, A. R. & Petraglia, F. (1999) *J. Clin. Endocrinol. Metab.* **84,** 2802–2806.
25. Jain, V., Vedernikov, Y. P., Saade, G. R., Chwalisz, K. & Garfield, R. E. (1999) *J. Pharmacol. Exp. Ther.* **288,** 407–413.
26. Jain, V., Longo, M., Ali, M., Saade, G. R., Chwalisz, K. & Garfield, R. E. (2000) *J. Soc. Gynecol. Invest.* **7,** 153–160.
27. Coste, S. C., Kesterson, R. A., Heldwein, K. A., Stevens, S. L., Heard, A. D., Hollis, J. H., Murray, S. E., Hill, J. K., Pantely, G. A., Hohimer, A. R., *et al*. (2000) *Nat. Genet.* **24,** 403–409.
28. Carmeliet, P., Ferreira, V., Breier, G., Pollefeyt, S., Kieckens, L., Gertsenstein, M., Fahrig, M., Vandenhoeck, A., Harpal, K., Eberhardt, C., *et al*. (1996) *Nature (London)* **380,** 435–439.
29. Ferrara, N., Carver-Moore, K., Chen, H., Dowd, M., Lu, L., O'Shea, K. S., Powell-Braxton, L., Hillan, K. J. & Moore, M. W. (1996) *Nature (London)* **380,** 439–442.
30. Chen, P. L., Scully, P., Shew, J. Y., Wang, J. Y. & Lee, W. H. (1989) *Cell* **58,** 1193–1198.
31. Lei, S., Richter, R., Bienert, M. & Mulvany, M. J. (1993) *Br. J. Pharmacol.* **108,** 941–947.
32. Rohde, E., Furkert, J., Fechner, K., Beyermann, M., Mulvany, M. J., Richter, R. M., Denef, C., Bienert, M. & Berger, H. (1996) *Biochem. Pharmacol.* **52,** 829–833.
33. Jain, V., Vedernikov, Y. P., Saade, G. R., Chwalisz, K. & Garfield, R. E. (1997) *Am. J. Obstet. Gynecol.* **176,** 234–240.
34. Parkes, D. G., Vaughan, J., Rivier, J., Vale, W. & May, C. N. (1997) *Am. J. Physiol.* **272,** H2115–H2122.
35. Turnbull, A. V., Vale, W. & Rivier, C. (1996) *Eur. J. Pharmacol.* **303,** 213–216.
36. Arbiser, J. L., Karalis, K., Viswanathan, A., Koike, C., Anand-Apte, B., Flynn, E., Zetter, B. & Majzoub, J. A. (1999) *J. Invest. Dermatol.* **113,** 838–842.
37. Giordano, F. J., Ping, P., McKirnan, M. D., Nozaki, S., DeMaria, A. N., Dillmann, W. H., Mathieu-Costello, O. & Hammond, H. K. (1996) *Nat. Med.* **2,** 534–539.
38. Hendel, R. C., Henry, T. D., Rocha-Singh, K., Isner, J. M., Kereiakes, D. J., Giordano, F. J., Simons, M. & Bonow, R. O. (2000) *Circulation* **101,** 118–121.
39. Schratzberger, P., Schratzberger, G., Silver, M., Curry, C., Kearney, M., Magner, M., Alroy, J., Adelman, L. S., Weinberg, D. H., Ropper, A. H. & Isner, J. M. (2000) *Nat. Med.* **6,** 405–413.